THE ASTROPHYSICAL JOURNAL, 637:L61–L64, 2006 January 20

PARTICLE ACCELERATION AND INTERMITTENT TURBULENCE IN CORONAL LOOPS

N. DÉCAMP[1] AND F. MALARA[1]

Received 2005 May 19; accepted 2005 December 14; published 2006 January 10

ABSTRACT

A test particle numerical experiment is performed to simulate particle acceleration in low-frequency turbulence generated by footpoint motions in a coronal loop. The turbulence is modeled within the reduced MHD theory. Only the effect of the resistive electric field $E_\parallel$ is retained, which is mainly parallel to the axial magnetic field. In its spectrum, the contribution of small scales is dominant. The spatial structure of $E_\parallel$ is obtained by a synthetic turbulence method (*p*-model), which allows us to reproduce intermittency. By solving the relativistic motion equations, the time evolution of particle distribution is calculated. Electrons can be accelerated to energies of the order of 50 keV in less than 0.3 s, and the final energy distribution can exhibit a power-law range. A correlation is found between the heating events in the MHD turbulence and particle acceleration that is qualitatively similar to what is observed in solar flares. Spatial intermittency plays a key role in acceleration, enhancing both the extension of a power-law range and the maximum energy.

Subject headings: acceleration of particles — Sun: flares — turbulence

1. INTRODUCTION

The acceleration of particles is one of the most relevant phenomena related to solar flares. Energetic particles carry up to 50% of the energy released in a flare (Miller et al. 1997; Saint-Hilaire & Benz 2002). Observations showed that during a flare, electrons can be accelerated to energies larger than 100 keV in times <1 s, and the energy spectra of hard X-ray emission display a single or double power-law range, often combined with a thermal component at lower energies (Holman 2003; Holman et al. 2003). Protons and other ions are accelerated up to energies larger than 1 MeV (e.g., Miller et al. 1997), and the γ-ray spectra also display a power-law range.

One difficulty in understanding the physics of such an efficient phenomenon is the large range of spatial scales involved: acceleration is probably due to kinetic effects at small scales, while the major source of energy of flares is in the large-scale magnetic structures, which can be described by magnetohydrodynamics (MHD). Models of particle acceleration are usually concerned with only part of the problem, and in many cases there is no relation between the energy release mechanism in a flare and particle acceleration. Different kinds of acceleration mechanisms have been considered in a number of papers: shock waves, MHD waves and turbulence, magnetic reconnection (see Miller et al. 1997 and Miller 1998 for a review), and "mixed" mechanisms in which turbulence is associated with a shock wave (Decker & Vlahos 1986) or with a current sheet (Ambrosiano et al. 1988).

Other models have been proposed with a more direct relation between acceleration and energy release events. Complex configurations with several acceleration sites where energy dissipation takes place are considered. These sites are small-scale current sheets, generated by the continuous shuffling of magnetic lines due to either photospheric motions or a nonlinear turbulent cascade. In the former case, the cellular automata technique has been used (Vlahos et al. 2004; Anastasiadis et al. 2004); in the latter case, turbulent electromagnetic fields have been reproduced either by direct MHD simulations (Dmitruk et al. 2003) or by other models (Arzner & Vlahos 2004). Turkmani et al. (2005) considered particle acceleration in direct three-dimensional MHD turbulence simulations in which footpoint motions are included. Such simulations describe more realistic topologies of the magnetic field, but the range of scales is limited. In particular, such simulations cannot describe that intermittency that appears at scales much smaller than the injection range of turbulence.

Intermittency can play a role in particle acceleration since it is responsible for intense localized velocity and magnetic field fluctuations, which can be related to intense electric fields. The effects of intermittency in coronal MHD turbulence has been studied by Nigro et al. (2004) using a shell technique applied to the reduced MHD (RMHD) equations. In this Letter we focus on the effects of intermittency in particle acceleration. We consider a model of synthetic turbulence that is intended to reproduce the turbulent fields in a coronal loop. The properties of such turbulence are derived from the RMHD shell model by Nigro et al. (2004). This allows us to directly relate particle acceleration to dissipative events in the time evolution of the turbulence.

2. THE MODEL

2.1. *Characterization of the Electric Field*

Our aim is to study the influence of the turbulent field properties on the acceleration process in a flare. As the magnetic field in a coronal loop is mainly longitudinal, we used the RMHD approximation (Strauss 1976): the longitudinal magnetic field $\boldsymbol{B}_0$ is uniform, the perpendicular to longitudinal magnetic field ratio is small ($\delta B_\perp \ll B_0$), and $\lambda_\parallel \gg \lambda_\perp$, with $\lambda_\parallel$ and $\lambda_\perp$ being the parallel and perpendicular wavelengths of the fluctuations. Within this approximation, perturbations propagate at the Alfvén speed $c_A = B_0/(4\pi\rho_0)^{1/2}$ (with ρ_0 being the uniform density) parallel and antiparallel to $\boldsymbol{B}_0$, while nonlinear couplings generate a turbulent cascade in the direction perpendicular to $\boldsymbol{B}_0$.

The electric field produced is described by

$$\boldsymbol{E} = -\frac{1}{c}\boldsymbol{v}\times\boldsymbol{B} + \eta\boldsymbol{j} = -\frac{1}{c}\boldsymbol{v}\times\boldsymbol{B} + \frac{c\eta}{4\pi}\boldsymbol{\nabla}\times\boldsymbol{B}, \quad (1)$$

with $\boldsymbol{v}$ being the velocity, $\boldsymbol{B}$ the magnetic field, $\boldsymbol{j}$ the current density, and η the resistivity. In the RMHD context, the velocity

[1] Dipartimento di Fisica, Università della Calabria, 87036 Rende (CS), Italy; decamp@fis.unical.it, malara@fis.unical.it.

TABLE 1
PARAMETERS OF THE MODEL

Parameter	$\delta v_{0\perp} = 14$ km s^{-1}	$\delta v_{0\perp} = 140$ km s^{-1}
$l_{D\perp} = c^{3/2}(\eta/4\pi\delta v_{0\perp})^{3/4} l_{0\perp}^{1/4}$	5.6 m	1 m
$l_{D\parallel} = (c_A c/\delta v_{0\perp}^{3/2})(\eta l_{0\perp}/4\pi)^{1/2}$	211 km	6.67 km
$\langle \delta E_\parallel(l_{D\parallel})\rangle = (\eta c/4\pi)(B_0/l_{D\parallel})$	4.5×10^{-5} V m^{-1}	1.41×10^{-3} V m^{-1}

and magnetic field fluctuations are perpendicular to $\boldsymbol{B}_0$: $\boldsymbol{v} = \delta v_\perp \boldsymbol{e}_\perp$, and $\boldsymbol{B} = B_0 \boldsymbol{e}_\parallel + \delta B_\perp \boldsymbol{e}_\perp$, with $\boldsymbol{e}_\parallel$ and $\boldsymbol{e}_\perp$ being unit vectors parallel and perpendicular, respectively, to $\boldsymbol{B}_0$. At the lowest order in the perturbation amplitude, the following electric field is found:

$$\boldsymbol{E} = -\frac{1}{c}\delta \boldsymbol{v}_\perp \times \boldsymbol{B}_0 + \frac{c\eta}{4\pi}\boldsymbol{\nabla}_\perp \times \delta \boldsymbol{B}_\perp = \delta \boldsymbol{E}_\perp + \delta \boldsymbol{E}_\parallel. \quad (2)$$

The perpendicular component $\delta \boldsymbol{E}_\perp$ of the electric field is responsible for particle drift, with the drift velocity being

$$\boldsymbol{u}_{\rm drift} = c\frac{\boldsymbol{E}\times\boldsymbol{B}}{B^2} \approx c\frac{\delta \boldsymbol{E}_\perp \times \boldsymbol{B}_0}{B_0^2} = \delta \boldsymbol{v}_\perp, \quad (3)$$

which corresponds to collective motions associated with the fluid velocity. Typical values of δv can be estimated from nonthermal line broadenings: $\delta v \lesssim 200$ km s^{-1} (Alexander et al. 1998; Mariska & McTiernan 1999; Harra et al. 2001). The particle acceleration is thus mainly governed by $\delta E_\parallel$, which is due to resistivity. We consider only this part of the electric field. Such a choice is also supported by the results of Turkmani et al. (2005, Fig. 4*b*), who found that particle distribution is mainly governed by the resistive electric field. As we shall see, the parallel velocity $u_\parallel$ of accelerated electrons can reach values much larger than $u_{\rm drift} \approx \delta v_\perp$. Thus, we considered only a one-dimensional particle motion in the direction parallel to $\boldsymbol{B}_0$.

As $\delta B_\perp$ and $\delta v_\perp$ exhibit power laws as a function of scale (e.g., Nigro et al. 2005), the same should hold for the resistive electric field. A range in the fluctuation spectra extending down to the dissipative scales is found, where $\delta B_\perp \sim B_0 \delta v_\perp / c_A$ (Nigro et al. 2005). In that range, the resistive electric field is $\delta \boldsymbol{E}_\parallel(l_\perp) = (c\eta/4\pi)\boldsymbol{\nabla}_\perp \times \delta \boldsymbol{B}_\perp \sim (c\eta B_0/4\pi c_A)(\delta v_\perp/l_\perp)$. Velocity fluctuations $\delta v_\perp(l_\perp)$ have a power-law spectrum $\delta v_\perp(l_\perp) = \delta v_\perp(l_{0\perp})\,(l_\perp/l_{0\perp})^\alpha$ of exponent $\alpha \sim \frac{1}{3}$, where $l_{0\perp}$ is the perpendicular injection scale. We thus obtain $\delta E_\parallel(l_\perp) = \delta E_\parallel(l_{0\perp})\,(l_\perp/l_{0\perp})^{\alpha-1}$. As $\alpha - 1 < 0$, we note that the resistive electric field is mainly due to the dissipative scales in the fluctuation spectrum.

In order to estimate the spectrum of $\delta E_\parallel$ as a function of $l_\parallel$, we consider the eddy turnover time defined by $\tau(l_\perp) = l_\perp/\delta v_\perp(l_\perp)$. Since the propagation of the perturbation occurs at the Alfvén speed in the parallel direction, the parallel length associated with this time is $l_\parallel = c_A\tau(l_\perp) = c_A l_\perp/\delta v_\perp(l_\perp)$, which can be written $\delta v_\perp(l_\perp)/l_\perp = c_A/l_\parallel$. Then we find the power law $\delta E_\parallel(l_\parallel) = c\eta B_0/(4\pi l_\parallel)$. The index is again negative (-1), which means that the small scales are the most important ones and that all associated phenomena (such as intermittency) are expected to play a major role. The smallest scale in this power-law range is the dissipative scale given by $l_{D\parallel} = l_{D\perp}[c_A/\delta v_\perp(l_{D\perp})]$, where $l_{D\perp}$ is the perpendicular dissipative scale. These quantities are expressed in Table 1. Since $u_\parallel \gg c_A$, the particle transit time $l_\parallel/u_\parallel$ across a given scale $l_\parallel$ is much smaller than the eddy turnover time $\tau(l_\perp) = l_\parallel/c_A$. Then the time dependence in the turbulent electric field will be neglected.

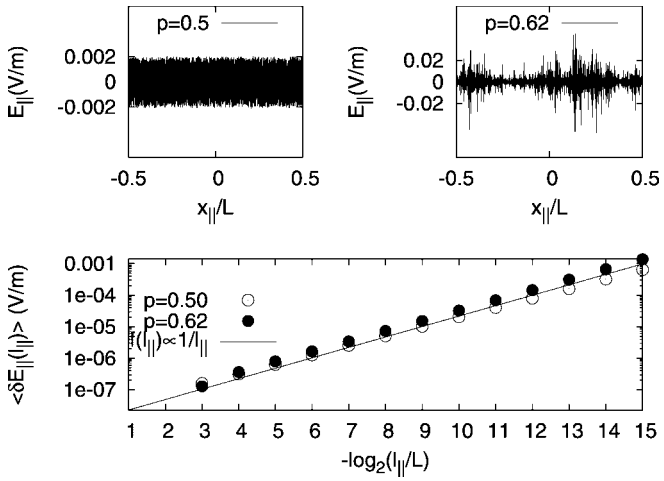

FIG. 1.—*Upper panels*: Electric field for $p = 0.5$ (without intermittency) and for $p = 0.62$. *Lower panel*: Corresponding spectra.

2.2. *The p-Model*

In order to reproduce an electric field with all the expected characteristics, we used a *p*-model (proposed by Meneveau & Sreenivasan 1987 and developed by Juneja et al. 1994). This model has the aim of reconstructing the spatial distribution of a field generated by a turbulent cascade. Its main advantage with respect to direct simulations is the possibility of accessing a wider range of scales, corresponding to a higher Reynolds number. We chose not to directly use a shell model because in that case, the field is obtained in a strongly simplified Fourier space, and the actual reconstruction methods are not able to reproduce, for example, the spatial intermittency of the field in the real space. In addition, in the *p*-model, the skewness, the scale index, and the degree (p) of intermittency are well controlled and easily adjustable.

The *p*-model is based on the local conservation of the energy flux. At one interval of size r, a coefficient is assigned, and this interval is then divided in two equal parts of size $r/2$. At one portion of the interval a fraction p of the parent coefficient is assigned, and at the other portion the rest of the parent coefficient $(1 - p)$ is assigned. This process is repeated at all the scales between the injection and the dissipative scales. The turbulent field is then obtained as a superposition of tent functions (basic wavelet functions) of different sizes and amplitudes. The amplitude of each tent is equal to the sum of all the coefficients corresponding to the same interval at a given power ($\frac{1}{3}$ for Kolmogorov, α in the generic case). Different realizations of the field are obtained by choosing a set of random numbers. We applied this method to calculate the electric field $\delta \boldsymbol{E}_\parallel$ with the power law obtained above. One example of such an electric field is plotted in Figure 1 for two different values of the intermittency parameter p: the field is statistically homogeneous for $p = 0.5$ (no intermittency), while it is dominated by spikes in the intermittent case ($p = 0.65$). In both cases, the spectrum is nearly the same.

Particle motion on this one-dimensional field is implemented assuming that $E_\parallel$ is constant in one cell of the model. The relativistic motion equations are solved analytically in each cell: $d[\gamma(u_\parallel)m_0 u_\parallel]/dt = qE_\parallel$ and $dx_\parallel/dt = u_\parallel$, where $\gamma(u_\parallel) = (1 - u_\parallel^2/c^2)^{-1/2}$, m_0 is the mass of the particle, and $L/2 \le x_\parallel \le L/2$ (with L being the loop length). These equations have been solved for a large number ($N = 2^{16}$) of particles. The initial position is randomly chosen in the range $[-L/2, L/2]$, while

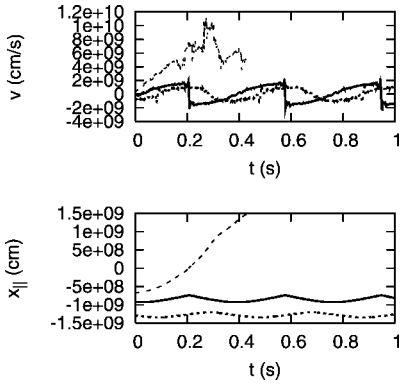

FIG. 2.—Time evolution of the velocity (*upper panel*) and position (*lower panel*) of two trapped particles (*dotted and solid lines*) and of one escaping particle (*dashed line*).

the initial velocity of the particles is derived from a thermal distribution. Since different particles can follow different magnetic field lines, we considered a different realization of $\delta E_{\parallel}(x_{\parallel})$ for each particle.

The values of the parameters of the model are loop length $L = 3 \times 10^9$ cm, Alfvén velocity $c_A = 6.4 \times 10^8$ cm s^{-1}, $B_0 \simeq 100$ G, density $n = 10^9$ cm^{-3}, perpendicular injection scale $l_{0\perp} = \pi \times 10^8$ cm, and initial temperature $T_0 = 1.5 \times 10^6$ K. Concerning the turbulent velocity, observations of the nonthermal broadening (Alexander et al. 1998; Mariska & McTiernan 1999; Harra et al. 2001) indicate that $\delta v_{0\perp}$ strongly increases during a flare. Thus, we considered two values: $\delta v_{0\perp} = 1.4 \times 10^6$ cm s^{-1} and $\delta v_{0\perp} = 1.4 \times 10^7$ cm s^{-1}, corresponding, respectively, to a "quiet" period and to an energy release event. We chose a resistivity $\eta = 1.3 \times 10^{-13}$ s. Such a value is many orders of magnitude smaller than what was used in direct MHD simulations (e.g., Turkmani et al. 2005), and it gives (for $\delta v_{0\perp} = 1.4 \times 10^7$ cm s^{-1}) a dissipation length $l_{D\perp}$ of the order of the proton Larmor radius r_L. On the other hand, $\eta \gg \eta_S$, where $\eta_S \sim 10^{-16}$ is the Spitzer resistivity. This corresponds to the idea that dissipation is not due to collisions but to kinetic effects, which are active at lengths $l_\perp \sim r_L$. The values of parallel $l_{D\parallel}$ and perpendicular $l_{D\perp}$ dissipative lengths are given in Table 1. Decreasing η gives both a smaller dissipative scale $l_{D\parallel}$ and lower values of the average $\delta E_{\parallel}$ at the scale $l_{D\parallel}$ [$\langle \delta E_{\parallel}(l_{D\parallel}) \rangle \propto \eta^{1/2}$]. On the other hand, with a smaller $l_{D\parallel}/l_{0\parallel}$ ratio, the effects of intermittency are enhanced: stronger spikes in $\delta E_{\parallel}$ are present. Thus, a small value of η yields a weak acceleration for most particles, leaving only a small minority interacting with the peaks of $\delta E_{\parallel}$ accelerated to high energies.

3. RESULTS

Due to the finite length L of the spatial domain, some particles escape from the domain, while others remain trapped inside potential wells associated with the electric field. This segregation process depends on the initial position and kinetic energy of the particles. The time evolution of some of the trapped and escaping particles is shown in Figure 2. However, transverse motions and the electric field time dependence are not included in the model. Adding such features, we expect that particle trapping would last for a finite time. In Figure 2, it is seen that the escaping particle considered exits the domain at the time $t \simeq 0.5$ s; we verified that this is the typical value of the escaping time.

In Figure 3, the energy distribution of electrons is plotted at

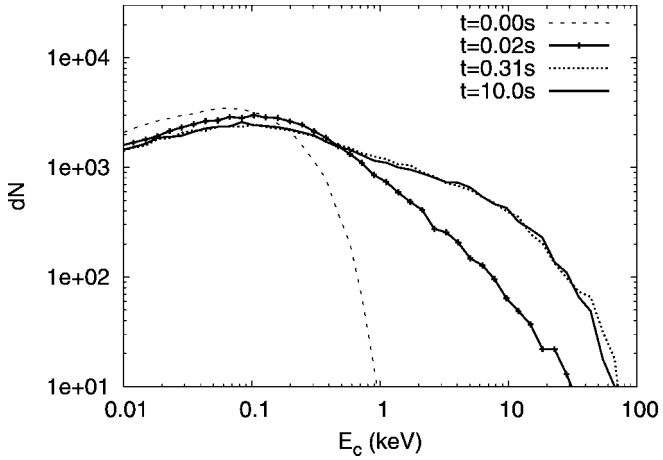

FIG. 3.—Evolution of the kinetic energy distribution as a function of time. The final distribution is reached in ~0.1 s

different times, in the case corresponding to a dissipative event ($\delta v_{0\perp} = 140$ km s^{-1}). Both escaping and trapped particles are included in the distribution. At times $t \sim 0.3$ s, the most energetic electrons attain energies ~50 keV, and the distribution approaches the final shape. After that time, the distribution remains essentially unchanged. The final distribution is formed by a quasi-thermal component, with a temperature slightly higher than T_0 and a power-law tail extending to energies ~50 keV.

In Figure 4, the final electron energy distribution is plotted for different $\delta v_{0\perp}$ and p. During a dissipative event ($\delta v_{0\perp} = 140$ km s^{-1}), particles are accelerated at energies much larger than in a quiet period ($\delta v_{0\perp} = 14$ km s^{-1}). Moreover, in the latter case, no power-law range is present. Thus, a correlation between dissipation in the MHD turbulence and particle acceleration clearly appears. Comparing the results of a nonintermittent ($p = 0.5$) electric field with those of an intermittent ($p = 0.62$, $p = 0.7$) electric field, we see that only in the latter case is a power-law range present. By increasing the degree p of intermittency, the power-law range becomes wider, and larger energies are reached.

The value of the Dreicer electric field is $E_D \simeq 1.6 \times 10^{-3}$ V m^{-1}, much larger than $\langle \delta E_{\parallel}(l_{D\parallel}) \rangle$ at $\delta v_{0\perp} = 14$ km s^{-1}. This reinforces the conclusion that no significant acceleration takes place during quiet periods. During an energy release event

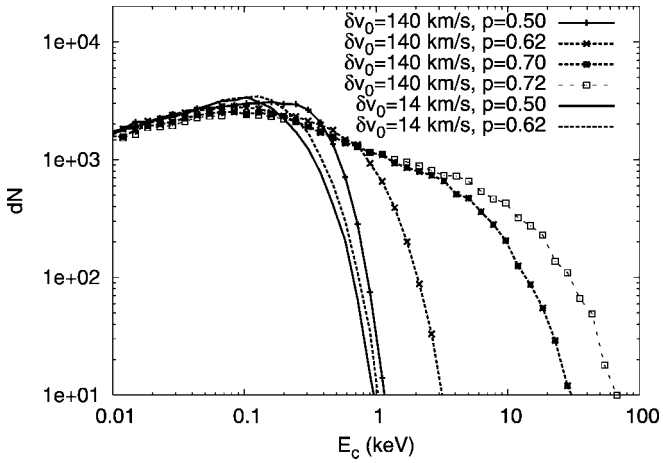

FIG. 4.—Correlation between heating, intermittency, and the final energy distribution. The particles are more accelerated with higher δv_0 and more intermittency.

($\delta v_{0\perp} = 140$ km s^{-1}), the average electric field $\langle \delta E_{\parallel}(l_{D\parallel}) \rangle$ is of the order of $E_{\rm D}$, but $E_{\parallel} \gg E_{\rm D}$ at intermittent peaks. Then we expect that collisions (not included in the model) would produce a thermalization of the distribution function at low energies while the high-energy tail would remain unaffected.

4. DISCUSSION AND CONCLUSIONS

In this Letter we have described a model of particle acceleration in a turbulent electric field, generated by low-frequency turbulence in a coronal structure with an intense magnetic field. The electric field considered is due to resistivity, and it is quasi-parallel to the background magnetic field. In the geometry considered, an inductive electric field only generates a particle drift corresponding to collective (fluid) motions, and it has been neglected. We derived the spectrum of the turbulent electric field as a function of the spectrum of the velocity perturbations from a RMHD shell model by Nigro et al. (2004). One important feature is that the main contribution to $E_{\parallel}$ comes from fluctuations at the smallest (dissipative) scale $l_{D\parallel}$. The spatial dependence of $E_{\parallel}$ as a function of $x_{\parallel}$ has been obtained by means of a synthetic turbulence technique, based on a *p*-model method.

The results of our model are that the MHD turbulence in a coronal loop is able to accelerate test particles to relativistic energies ($\sim 5 \times 10^4$ eV) in a relatively short time ($\sim$0.3 s for electrons) even with an extremely small value for the resistivity. In such a case, the average electric field is too small to produce a significant acceleration. On the contrary, the strong spikes due to intermittency are responsible for the formation of the high-energy tail. This fact shows the key role played by intermittency in this process. We stress that such phenomena are due to the very low values of the resistivity η, which are not accessible to direct MHD simulations. The efficiency of the acceleration process is related to the rms (fluid) velocity fluctuation $\delta v_{0\perp}$: larger values of such a parameter give larger acceleration. Nigro et al. (2005) have shown that an increase in the turbulent velocity $\delta v_{0\perp}$ is related to the dissipative events in which the plasma is heated by the turbulent cascade. Thus, our model is able to reproduce a correlation between plasma heating and particle acceleration (with consequent hard X-ray emission) during a flare. We did not evaluate the fraction of the total flare energy released in accelerated particles; however, we expect this efficiency to be small as turbulent models are more adapted to the description of microflares. Moreover, the model does not accelerate all the electrons of the loop (as observed by Hoyng et al. 1976), and the fraction of electrons accelerated in nonthermal tails is small.

While several important ingredients are included in the model, it is based on a very simplified one-dimensional geometry, and other physical features have been neglected. Thus, it should be considered as a first step toward a more detailed modeling of the phenomenon. In the future, we plan to include the effect of collisions, another spatial dimension, and the time dependence of the turbulent fields.

The authors thank L. Vlahos and H. Isliker for their useful discussions. This work was funded by the European Commission under research training network HPRN-CT-2001-00310.

REFERENCES

Alexander, D., Harra-Murnion, L. K., Khan, J. I., & Matthews, S. A. 1998, ApJ, 494, L235
Ambrosiano, J., Matthaeus, W. H., Goldstein, M. L., & Plante, D. 1988, J. Geophys. Res., 93, 14383
Anastasiadis, A., Gontikakis, G., Vilmer, N., & Vlahos, L. 2004, A&A, 422, 323
Arzner, K., & Vlahos, L. 2004, ApJ, 605, L69
Decker, R. B., & Vlahos, L. 1986, ApJ, 306, 710
Dmitruk, P., Matthaeus, W. H., Seenu, N., & Brown, M. R. 2003, ApJ, 597, L81
Harra, L. K., Matthews, S. A., & Culhane, J. L. 2001, ApJ, 549, L245
Holman, G. D. 2003, ApJ, 586, 606
Holman, G. D., Sui, L., Schwartz, R. A., & Emslie, A. G. 2003, ApJ, 595, L97
Hoyng, P., van Beek, H. F., & Brown, J. C. 1976, Sol. Phys., 48, 197
Juneja, A., Lathrop, D. P., Sreenivasan, K. R., & Stolovitsky, G. 1994, Phys. Rev. E, 49, 5179
Mariska, J. T., & McTiernan, J. M. 1999, ApJ, 514, 484
Meneveau, C., & Sreenivasan, K. R. 1987, Phys. Rev. Lett., 59, 1424
Miller, J. A. 1998, Space Sci. Rev., 86, 79
Miller, J. A., et al. 1997, J. Geophys. Res., 102, 14631
Nigro, G., Malara, F., Carbone, V., & Veltri, P. 2004, Phys. Rev. Lett., 92, 194501
Nigro, G., Malara, F., & Veltri, P. 2005, ApJ, 629, L133
Saint-Hilaire, P., & Benz, A. O. 2002, Sol. Phys., 210, 287
Strauss, H. R. 1976, Phys. Fluids, 19, 134
Turkmani, R., Vlahos, L., Galsgaard, K., Cargill, P. J., & Isliker, H. 2005, ApJ, 620, L59
Vlahos, L., Isliker, H., & Lepreti, F. 2004, ApJ, 608, 540